Analytical Studies of Isothermal Sphere Collapse

Evangelia Ntormousi
Project Supervisor: Patrick Hennebelle
Collaborators: Chris Matzner, Pascale Garaud, Matthias Gritschneder

1. Introduction

It has been known for a long time that most stars form in binary systems and that, in general, stars are preferably found in multiple systems. However, the processes responsible for the formation of multiple stellar systems are still under debate and reproducing the properties of binary systems is a challenge for any theory of star formation (Goodwin et al. 2007).

According to our current view of star formation, cores in a molecular cloud become gravitationally unstable and collapse to form the first stellar objects. The physical conditions in a molecular cloud, such as turbulence, will then determine the outcome of star formation from these cores (Elmegreen & Scalo 2004; Chabrier & Hennebelle 2010). Evidence for this can, for instance, be found in the fact that the distribution of core masses in a cloud, usually called the Core Mass Function (CMF), has been found to resemble the stellar mass distribution, or Initial Mass Function (IMF) (Matzner & McKee 2000; Alves et al. 2007).

In fact, simulations of gravitational collapse of pre-stellar cores have shown that the initial density profile of a core and potential velocity perturbations in its interior due to turbulent motions will lead to fragmentation and to the formation of many protostellar objects (Bate & Bonnell 2005; Girichidis et al. 2011). This view of core fragmentation during the first phases of the gravitational collapse is also supported by observations Maury et al. (2010). In view of these numerical and observational facts, it is very relevant to study the fragmentation of a pre-stellar core analytically, in order to isolate the nature of perturbations that could grow to break a core up into smaller objects.

Naturally, the gravitational collapse of a core has been studied analytically since very early on. Larson (1969) and Penston (1969) published their results of the analytical study of the collapse of an isothermal sphere almost simulataneously, providing a solution to the hydrodynamics equations that is now called the Larson-Penston collapse solution. Shu (1977) extended their work to obtain a whole family of solutions for this problem, which all have the particularly interesting characteristic of self-similarity. The Larson-Penston solution also belongs to this family of solutions, although it suffers from the existence of a critical point, which in this case is an unphysical feature.

Hanawa & Matsumoto (1999), hereafter HM99, and Hanawa & Matsumoto (2000) explored the dispersion relation of a linear perturbation to the Larson-Penston flow in the form of spherical harmonics. They found that for an isothermal equation of state, the l=2 perturbation mode has

a growth rate $\sigma \simeq 0.325$, finding no higher unstable modes. This problem involves the numerical integration of a system of coupled ordinary differential equations as an eigenvalue problem for each perturbation mode. The perturbation equations contain the equilibrium solution, which then also defines the boundary conditions of the problem. That work was however limited to exponentially growing modes only and the eigenvalue problem was treated with a shooting method, which is very sensitive to numerical accuracy issues. Moreover, as mentioned above, the Larson-Penston solution has an inherent critical point, a fact that makes numerical integration problematic.

The aim of this project is to to continue the work of HM99 by imposing a linear perturbation to a self-similar collapse solution and, as a first step, looking at the complete perturbation, including the oscillatory modes as well as the exponentially growing modes. The following step would be to apply the perturbation to the more general Shu family of solutions. Eventually, we would like to compare our analytical findings to numerical simulations of the same initial setup.

This is a progress report, containing the results of this work up to this date. In Section 2 we present the derivation of the perturbation equations. In section 3 we present the Larson-Penston and the Shu equilibrium solutions. Section 4 summarizes the different numerical approaches for solving the system perturbation equations. Our results so far are presented in Section 5 and we present the following steps for concluding this project in Section 6.

2. Derivation of the perturbation equations

2.1. Perturbation including exponential modes only

The equations of hydrodynamics in spherical coordinates are:

$$
\begin{aligned}
\frac{\partial \rho}{\partial t} + \frac{1}{r^2}\frac{\partial}{\partial r}(r^2 \rho u_r) + \frac{1}{r sin\theta}\frac{\partial}{\partial \theta}(sin\theta \rho u_\theta) + \frac{1}{r sin\theta}\frac{\partial}{\partial \phi}(\rho u_\phi) &= 0 \\
\frac{\partial u_r}{\partial t} + u_r\frac{\partial u_r}{\partial r} + \frac{u_\theta}{r}\frac{\partial u_r}{\partial \theta} + \frac{u_\phi}{r sin\theta}\frac{\partial u_r}{\partial \phi} - \frac{u_\phi^2 + u_\theta^2}{r} &= -\frac{1}{\rho}\frac{\partial \rho}{\partial r} - \frac{\partial \Psi}{\partial r} \\
\frac{\partial u_\theta}{\partial t} + u_r\frac{\partial u_\theta}{\partial r} + \frac{u_\theta}{r}\frac{\partial u_\theta}{\partial \theta} + \frac{u_\phi}{r sin\theta}\frac{\partial u_\theta}{\partial \phi} + \frac{u_r u_\theta}{r} - \frac{u_\phi^2}{r tan\theta} &= -\frac{1}{r\rho}\frac{\partial \rho}{\partial \theta} - \frac{1}{r}\frac{\partial \Psi}{\partial \theta} \\
\frac{\partial u_\phi}{\partial t} + u_r\frac{\partial u_\phi}{\partial r} + \frac{u_\theta}{r}\frac{\partial u_\phi}{\partial \theta} + \frac{u_\phi}{r sin\theta}\frac{\partial u_\phi}{\partial \phi} + \frac{u_r u_\phi}{r} &= -\frac{1}{r\rho sin\theta}\frac{\partial \rho}{\partial \phi} - \frac{1}{r sin\theta}\frac{\partial \Psi}{\partial \phi} \\
\frac{1}{r^2}\frac{\partial}{\partial r}\left(r^2\frac{\partial}{\partial r}\right)\Psi + \frac{1}{r^2 sin\theta}\frac{\partial}{\partial \theta}\left(sin\theta\frac{\partial}{\partial \theta}\right)\Psi + \frac{1}{r^2 sin^2\theta}\frac{\partial^2}{\partial \phi^2}\Psi &= 0 \qquad (1)
\end{aligned}
$$

We apply a perturbation of the form:

$$
\begin{aligned}
\rho(r,t) &= \frac{R(x)}{t^2} + t^{\sigma-2} r_1(x) Y_l^m = \rho_0 + \delta\rho \\
u_r(r,t) &= u(x) + t^{\sigma} u_{1r}(x) Y_l^m = u_{r0} + \delta u_r \\
u_\theta(r,t) &= \frac{1}{l+1} t^{\sigma} u_{1\theta}(x) \frac{\partial Y_l^m}{\partial \theta} = \delta u_\theta \\
u_\phi(r,t) &= \frac{1}{l+1} \frac{1}{sin\theta} t^{\sigma} u_{1\theta}(x) \frac{\partial Y_l^m}{\partial \phi} = \delta u_\phi \\
\Psi(r,t) &= \Psi_0(x) + t^{\sigma} \Phi_1(x) Y_l^m = \Psi_0 + \delta\Phi
\end{aligned} \tag{2}
$$

where $x = r/t$ is the similarity variable used for this calculation, σ is the eigenvalue and Y_l^m are the spherical harmonics. R(x) and u(x) are the equilibrium density and velocity as a function of x and all quantities with the subscript 1 represent the perturbation dependence on x.

Inserting the perturbations 2 in equations 1 we get the following, neglecting second-order terms:

From the equation of continuity:

$$\begin{aligned}
\frac{\partial}{\partial t}(\rho_0+\delta_\rho)+\frac{1}{r^2}\frac{\partial}{\partial r}(r^2(\rho_0+\delta\rho)(u_{r0}+\delta u_r)) &+\\
\frac{1}{rsin\theta}\frac{\partial}{\partial\theta}(sin\theta(\rho_0+\delta\rho)\delta u_\theta) &+\\
\frac{1}{rsin\theta}\frac{\partial}{\partial\phi}((\rho_0+\delta\rho)\delta u_\phi) &= 0\Rightarrow\\
\frac{\partial\delta\rho}{\partial t}+\frac{1}{r^2}\frac{\partial}{\partial r}(r^2\rho_0\delta u_r+r^2\delta\rho u_{r0}) &+\\
\frac{1}{rsin\theta}\frac{\partial}{\partial\theta}(sin\theta\rho_0\delta u_\theta)+\frac{1}{rsin\theta}\frac{\partial}{\partial\phi}(\rho_0\delta u_\phi) &= 0\Rightarrow\\
\frac{\partial}{\partial t}\left(t^{\sigma-2}r_1(x)Y_l^m\right) &+\\
\frac{1}{x^2t^3}\frac{d}{dx}\left(x^2R(x)t^\sigma u_{1r}(x)Y_l^m+x^2t^\sigma r_1(x)Y_l^m u(x)\right) &+\\
\frac{1}{xtsin\theta}\left(cos\theta\rho_0\delta u_\theta+sin\theta\rho_0\frac{\partial\delta u_\theta}{\partial\theta}\right) &+\\
\frac{1}{rsin\theta}\left(\rho_0\frac{\partial\delta u_\phi}{\partial\phi}\right) &= 0\Rightarrow\\
(\sigma-2)t^{\sigma-3}r_1(x)Y_l^m-\frac{x}{t}t^{d-2}\frac{dr_1}{dx} &+\\
\frac{1}{x^2t^3}\frac{d}{dx}\left(x^2R(x)t^\sigma u_{1r}(x)Y_l^m+x^2t^\sigma r_1Y_l^m u(x)\right) &+\\
\frac{1}{xtsin\theta}\left(cos\theta\rho_0\delta u_\theta+sin\theta\rho_0\frac{\partial\delta u_\theta}{\partial\theta}\right) &+\\
\frac{1}{rsin\theta}\left(\rho_0\frac{\partial\delta u_\phi}{\partial\phi}\right) &= 0\Rightarrow\\
(\sigma-2)t^{\sigma-3}r_1(x)Y_l^m-xt^{\sigma-3}\frac{dr_1}{dx}Y_l^m &+\\
\frac{1}{x^2t^3}\left(2xR(x)t^\sigma u_{1r}Y_l^m+x^2\frac{dR}{dx}t^\sigma u_{1r}Y_l^m+x^2R(x)t^\sigma\frac{du_{1r}}{dx}Y_l^m+2xt^\sigma r_1uY_l^m\right) &+\\
\frac{cotan\theta}{xt}\rho_0\delta u_\theta+\frac{1}{xt}\rho_0\frac{\partial\delta u_\theta}{\partial\theta} &+\\
\frac{1}{xtsin\theta}\rho_0\frac{\partial\delta u_\phi}{\partial\phi} &= 0\Rightarrow
\end{aligned}$$

$$
\begin{aligned}
(\sigma-2)r_1(x)Y_l^m - x\frac{dr_1}{dx}Y_l^m + \frac{2}{x}R(x)u_{1r}Y_l^m + \frac{dR}{dx}u_{1r}Y_l^m &+ \\
R(x)\frac{du_{1r}}{dx}Y_l^m + \frac{2}{x}r_1(x)u(x)Y_l^m + \frac{dr_1}{dx}u(x)Y_l^m + r_1\frac{du}{dx}Y_l^m &+ \\
\frac{cotan\theta}{xt}\frac{R}{t^2}\frac{1}{l+1}u_{1\theta}\frac{\partial Y_l^m}{\partial\theta} &+ \\
\frac{1}{xt}\frac{R}{t^2}\frac{1}{l+1}u_{1\theta}\frac{\partial^2 Y_l^m}{\partial\theta^2} &+ \\
\frac{1}{xtsin\theta}\frac{R}{t^2}\frac{1}{l+1}\frac{1}{sin\theta}u_{1\theta}\frac{\partial^2 Y_l^m}{\partial\phi^2} &= 0 \\
(\sigma-2)r_1(x)Y_l^m - x\frac{dr_1}{dx}Y_l^m + \frac{2}{x}R(x)u_{1r}Y_l^m + \frac{dR}{dx}u_{1r}Y_l^m &+ \\
R(x)\frac{du_{1r}}{dx}Y_l^m + \frac{2}{x}r_1(x)u(x)Y_l^m + \frac{dr_1}{dx}u(x)Y_l^m + r_1(x)\frac{du}{dx}Y_l^m &+ \\
\frac{R(x)u_{1\theta}}{x(l+1)}\left(cotan\theta\frac{\partial Y_l^m}{\partial\theta} + \frac{\partial^2 Y_l^m}{\partial\theta^2} + \frac{1}{sin^2\theta}\frac{\partial^2 Y_l^m}{\partial\phi^2}\right) &= 0
\end{aligned}
$$

If we replace $\nabla^2 Y_l^m = \left(\frac{\partial^2 Y_l^m}{\partial\theta^2} + cotan\theta\frac{\partial Y_l^m}{\partial\theta} + \frac{1}{sin^2\theta}\frac{\partial^2 Y_l^m}{\partial\phi^2}\right) = -l(l+1)Y_l^m$, from the definition of the spherical harmonics, we have

$$
(u(x)-x)\frac{dr_1}{dx} + R\frac{du_{1r}}{dx} + \left(\sigma - 2 + \frac{2u(x)}{x} + \frac{du}{dx}\right) + \left(\frac{2R}{x} + \frac{dR}{dx}\right)u_{ir} - \frac{lR}{x}u_{1\theta} = 0 \qquad (3)
$$

Putting the pertubations 2 in the radial momentum equation gives:

$$
\begin{aligned}
\frac{\partial}{\partial t}(u_{0r}+\delta u_r) + (u_{r0}+\delta u_r)\frac{\partial}{\partial r}(u_{r0}+\delta u_r) &+ \\
\frac{\delta u_\theta}{r}\frac{\partial}{\partial\theta}(u_{r0}+\delta u_r) &+ \\
\frac{\delta u_\phi}{rsin\theta}\frac{\partial}{\partial\phi}(u_{r0}+\delta u_r) &= \\
-\frac{1}{\rho_0+\delta\rho}\frac{\partial}{\partial r}(\rho_0+\delta\rho) - \frac{1}{rsin\theta}\frac{\partial}{\partial\theta}(\Psi_0+\delta\Phi) &\Rightarrow
\end{aligned}
$$

$$\begin{aligned}
\frac{\partial \delta u_r}{\partial t} + \delta u_r \frac{\partial u_{r0}}{\partial r} \quad &+ \\
u_{r0} \frac{\partial \delta u_r}{\partial r} \quad &= \\
-\frac{1}{\rho_0}\frac{\partial \delta\rho}{\partial r} + \frac{1}{\rho_0^2}\delta\rho\frac{\partial \rho_0}{\partial r} \quad &\Rightarrow \\
\frac{\partial}{\partial t}\left(t^\sigma u_{1r}(x) Y_l^m\right) + \left(t^\sigma u_{1r} Y_l^m\right)\frac{du}{dx}\frac{1}{t} \quad &+ \\
u(x) t^{\sigma-1}\frac{du_{1r}}{dx} Y_l^m \quad &= \\
-\frac{t^2}{R(x)}\frac{d}{dx}\left(t^{\sigma-2} r_1 Y_l^m\right)\frac{1}{t} \quad &- \\
\frac{t^4}{R^2}\left(t^{\sigma-2} r_1 Y_l^m\right)\frac{d}{dx}\left(\frac{R}{t^2}\right)\frac{1}{t} \quad &- \\
\frac{d}{dx}\left(t^\sigma \Phi_1 Y_l^m\right)\frac{1}{t} \quad &\Rightarrow
\end{aligned}$$

$$\frac{1}{R}\frac{dr_1}{dx} + (u(x)-x)\frac{du_{1r}}{dx} - \left(\frac{1}{R^2}\frac{dR}{dx}\right) r_1 + \left(d + \frac{du}{dx}\right) u_{1r} + \frac{d\Phi_1}{dx} = 0 \tag{4}$$

Similarly, from the other two momentum equations we get the relation (the same for ϕ and θ):

$$(u(x)-x)\frac{du_{1\theta}}{dx} + \left(\frac{u}{x} + d\right) u_{1\theta} + (l+1)\frac{1}{xR} r_1 + \frac{l+1}{x}\Phi_1 = 0 \tag{5}$$

And from the equation for the potential:

$$\frac{d^2\Phi_1}{dx^2} + \frac{2}{x}\frac{d\Phi_1}{dx} - \frac{l(l+1)}{x^2}\Phi_1 = r_1 \tag{6}$$

We combine equations 3 and 4 to eliminate $\frac{du_{1r}}{dx}$, by multiplying 3 by $(u-x)$ and 4 by R and subtracting. The we get:

$$\begin{aligned}
\left[(u-x)^2 - 1\right]\frac{dr_1}{dx} + \left[\left(\sigma - 2 + \frac{2u}{x} + \frac{du}{dx}\right)(u-x) + \frac{1}{R}\frac{dR}{dx}\right] r_1 \quad &+ \\
\left[\left(\frac{2R}{x}\frac{dR}{dx}\right)(u-x) - R\left(d + \frac{du}{dx}\right)\right] u_{1r} - \frac{lR}{x}(u-x) u_{1\theta} - R\frac{d\Phi}{dx} \quad &= \quad 0
\end{aligned} \tag{7}$$

Equations 4, 5, 6 and 7 can be integrated to give the space dependence of the perturbations as the core collapses.

2.2. Derivation of the full perturbation equations

Following the same process described in the previous section, we can derive the perturbation equations including the oscillatory modes as well. Then the perturbation will have the form:

$$\begin{aligned}
\rho(r,t) &= \frac{R(x)}{t^2} + t^{\sigma-2}Y_l^m\left(r_1(x)\cos\omega\ln t + r_2(x)\sin\omega t\right) = \rho_0 + \delta\rho \\
u_r(r,t) &= u(x) + t^{\sigma}u_{1r}(x)Y_l^m\left(u_{1r}(x)\cos\omega\ln t + u_{2r}(x)\sin\omega t\right) = u_{r0} + \delta u_r \\
u_\theta(r,t) &= \frac{1}{l+1}t^{\sigma}u_{1\theta}(x)\frac{\partial Y_l^m}{\partial\theta}\left(u_{1\theta}(x)\cos\omega\ln t + u_{2\theta}(x)\sin\omega t\right) = \delta u_\theta \\
u_\phi(r,t) &= \frac{1}{l+1}\frac{1}{sin\theta}t^{\sigma}u_{1\theta}(x)\frac{\partial Y_l^m}{\partial\phi}\left(u_{1\theta}(x)\cos\omega\ln t + u_{2\theta}(x)\sin\omega t\right) = \delta u_\phi \\
\Psi(r,t) &= \Psi_0(x) + t^{\sigma}\Phi_1(x)Y_l^m\left(\Phi_1(x)\cos\omega\ln t + \Phi_2(x)\sin\omega t\right) = \Psi_0 + \delta\Phi
\end{aligned} \tag{8}$$

where ω is the frequency of the oscillation.

The system of equations we derive then will be the same as before, with a few coupling terms between the two components of the oscillatory perturbation:

$$\begin{aligned}
(u(x)-x)\frac{dr_1}{dx} &+ R\frac{du_{1r}}{dx} + \left(\frac{2R}{x}+\frac{dR}{dx}\right)u_{1r} + \\
\left(\frac{2u}{x}+\frac{du}{dx}+\sigma-2\right)r_1 + \omega r_2 - \frac{lR}{x}u_{1\theta} &= 0 \\
(u(x)-x)\frac{dr_2}{dx} &+ R\frac{du_{2r}}{dx} + \left(\frac{2R}{x}+\frac{dR}{dx}\right)u_{2r} + \\
\left(\frac{2u}{x}+\frac{du}{dx}+\sigma-2\right)r_2 - \omega r_1 - \frac{lR}{x}u_{2\theta} &= 0 \\
\frac{1}{R}\frac{dr_1}{dx} &+ (u(x)-x)\frac{du_{1r}}{dx} + \left(\sigma+\frac{du}{dx}\right)u_{1r} + \\
\omega u_{2r} - \frac{1}{R^2}\frac{dR}{dx}r_1 + \Phi_1 &= 0 \\
\frac{1}{R}\frac{dr_2}{dx} &+ (u(x)-x)\frac{du_{2r}}{dx} + \left(\sigma+\frac{du}{dx}\right)u_{2r} - \\
\omega u_{1r} - \frac{1}{R^2}\frac{dR}{dx}r_2 + \Phi_2 &= 0 \\
(u(x)-x)\frac{du_{1\theta}}{dx} &+ u_{1\theta} + \omega u_{2\theta} + \frac{\Phi_1}{x} = 0 \\
(u(x)-x)\frac{du_{2\theta}}{dx} &+ u_{2\theta} - \omega u_{1\theta} + \frac{\Phi_2}{x} = 0 \\
\frac{d^2\Phi_1}{dx^2} &+ \frac{2}{x}\frac{d\Phi_1}{dx} - \frac{l(l+1)}{x^2} = r_1 \\
\frac{d^2\Phi_2}{dx^2} &+ \frac{2}{x}\frac{d\Phi_2}{dx} - \frac{l(l+1)}{x^2} = r_2
\end{aligned}$$

3. Equilibrium solutions

The equilibrium solutions to which we can apply the perturbation should be self-similar gravitational collapse solutions. As already mentioned in the Introduction, a family of such solutions (time-reversable to give self-gravitating winds) were derived by Shu (1977), after Larson (1969) and Penston (1969) published their collapse solution, which is a special case of the Shu family of solutions. Below we summarize the characteristics of such solutions.

3.1. The Shu solutions

We imagine a spherical core which is collapsing to a central object. For a spherically symmetric flow we can write the equation for mass conservation in terms of spherical mass shells:

$$\begin{aligned} \frac{\partial M}{\partial t} + u\frac{\partial M}{\partial r} &= 0 \\ \frac{\partial M}{\partial r} &= 4\pi r^2 \rho \end{aligned} \tag{9}$$

where M(r) is the total mass contained in a shell of radius r. If α is the isothermal sound speed, the force equation can be written as:

$$\frac{\partial u}{\partial t} + u\frac{\partial u}{\partial r} = -\frac{\alpha}{\rho}\frac{\partial \rho}{\partial r} - \frac{GM}{r^2} \tag{10}$$

By introducing the similarity variable $x = r/\alpha t$ and substituting solutions of the form:

$$\rho(r,t) = \frac{\alpha(x)}{4\pi G t^2} \tag{11}$$

$$M(r,t) = \frac{\alpha^2 t}{G} m(x) \tag{12}$$

$$u(r,t) = \alpha u(x) \tag{13}$$

into equations 9 and 10 we get, after some manipulation,

$$\begin{aligned} \left[(x-u)^2 - 1\right]\frac{du}{dx} &= \left[\alpha(x-u) - \frac{2}{x}\right](x-u) \\ \left[(x-u)^2 - 1\right]\frac{1}{\alpha}\frac{d\alpha}{dx} &= \left[\alpha - \frac{2}{x}(x-u)\right](x-u) \end{aligned} \tag{14}$$

and

$$m = x^2 \alpha (x - u) \tag{15}$$

The solutions to these equations will give the space and time dependence of the flow during the collapse of an isothermal gas sphere. Figure 1 shows the dependence of velocity on the similarity variable, x.

There exists an exact analytic solution to equations 14, which is the static case:

$$\begin{aligned} u &= 0 \\ \alpha &= \frac{2}{x^2} \\ m &= 2x \end{aligned} \tag{16}$$

and is actually the hydrostatic case of a singular isothermal sphere. Another solution, which appears to be also a singular solution to equations 14 is

$$\begin{aligned} x - u &= 1 \\ \alpha &= \frac{2}{x} \end{aligned}$$

However, as explained in Shu (1977), this kind of solutions which contain critical points are not generally acceptable solutions for the collapse of an isothermal sphere. A special case of a solution with a critical point is the Larson-Penston collapse solution. Although this type of solution can be argued to be an inadequate description of this problem, we consider it here for continuity with the work of HM99.

3.2. The Larson-Penston solution

As mentioned before, the Larson-Penston solution was published before Shu's more complete analysis of the isothermal sphere collapse problem. By starting from the boundary conditions:

$$\begin{aligned} u &\rightarrow \frac{2}{3} x \\ \alpha &\rightarrow 1.67 \\ m &\rightarrow 0.56 x^3 \end{aligned}$$

at $x \rightarrow 0$ and integrating equations 14 with a simple fourth-order Runge-Kutta scheme, we obtain the Larson-Penston solution, shown in Figure 2.

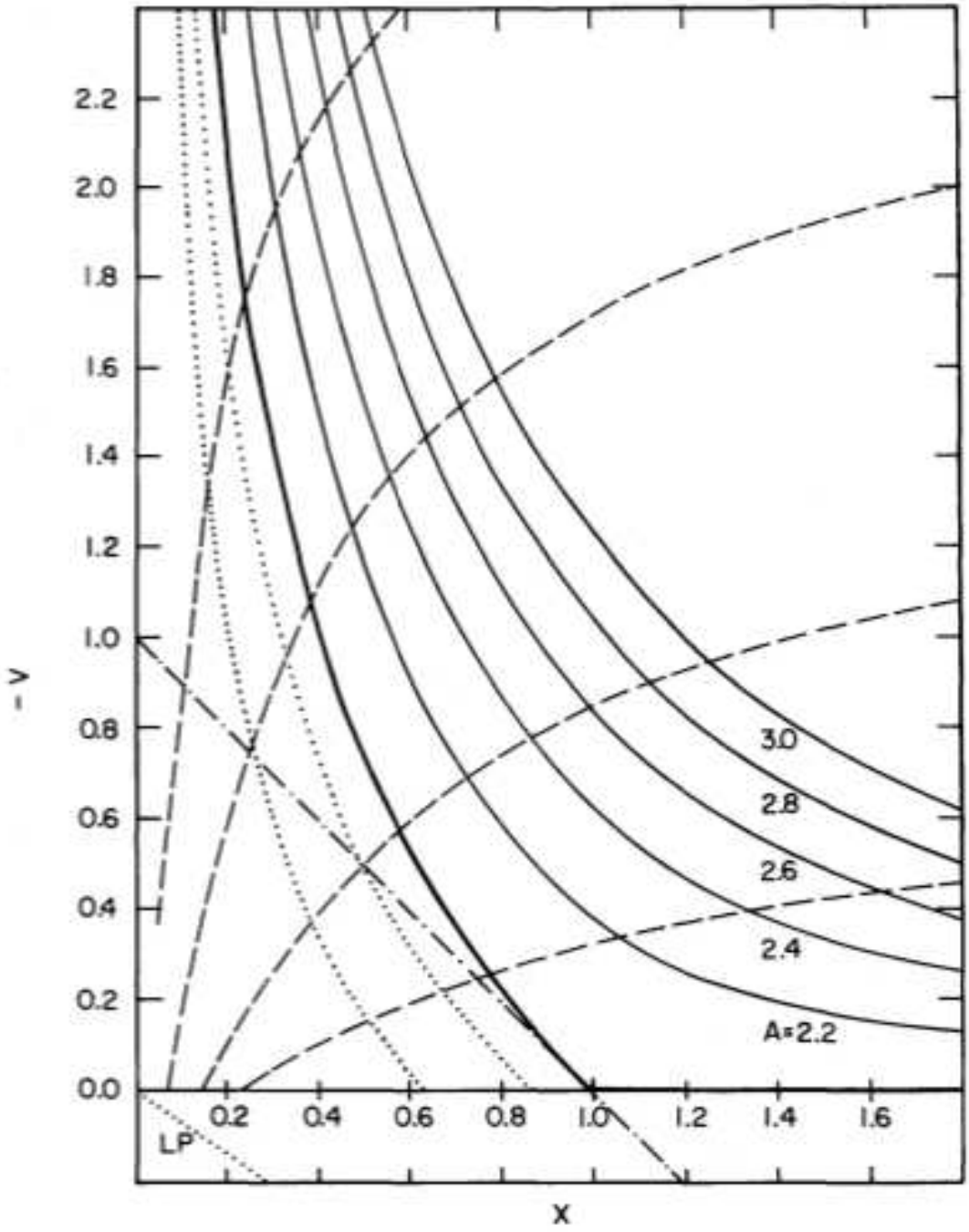

Fig. 1.— The Shu similarity solutions (Figure 2 of Shu (1977)). The dotted-dashed line shows the locus of the critical points. The small dotted line at the bottom is the Larson-Penston solution.

4. Numerical Integration of the equations

Having derived the perturbation equations analytically and chosen an equilibrium solution to which we want to apply the perturbation, finding the dispersion relation between the perturbation mode l (the equations are degenerate to the m of the spherical harmonics) and the growth rate of the perturbation is a matter of integrating the system of perturbation equations. Unfortunately, it is not possible to solve this system analytically for a complex case, so the eigenvalue problem for each perturbation mode should be solved numerically.

A simple test case for each method that can be solved analytically is the one of a constant perturbation, of the form

$$\begin{aligned} r_1 &= c_1 \\ u_{r1} &= c_2 x \\ u_{\theta 1} &= 0 \\ \Phi_1 &= c_1 x^2/6 \end{aligned}$$

applied to an unphysical, but simple equilibrium solution to equations 14:

$$\begin{aligned} R &= 2/3 \\ u &= 2x/3 \end{aligned}$$

for which we can easily derive σ for the restricted perturbation equations and for l=0 to be $\sigma_\pm = -1, 2/3$.

The first step to our analysis is to reproduce the work of HM99, using the Larson-Penston solution as an equilibrium solution and only looking at the growing perturbations.

In order to make sure that our analysis converges to the true eigenvalue of the problem and to test for the stability of our method we have tried different methods for solving the eigenvalue problem, the principles of each we discuss in the following.

4.1. A shooting method

This is the method used in HM99. It consists in integrating two different boundary conditions from $x \to 0$ to infinity, and looking for a value of σ such that the solution satisfies the boundary conditions at infinity.

For the Larson-Penston flow the asymptotic form of the solution near x=0 is:

$$\begin{aligned} r_1 &= c_1 x^l \\ u_{r1} &= c_2 x^{l-1} \\ u_{\theta 1} &= c_2 (l+1) x^{l-1}/l \\ \Phi_1 &= (-c_1/\rho_0 - (\sigma + 1 - l/3) c_2) x^l \end{aligned}$$

where ρ_0 is the value of the Larson-Penston solution close to x=0.

Since the equilibrium solution has a critical point, it is not possible to integrate directly from x=0 to infinity (in fact, a very large number for the sake of the numerical computation). What we do instead is to integrate from zero to a value of x just before the critical point ($x = x_{crit} - dx$), for two linearly independent solution vectors, and then find a linear combination of these solutions to satisfy the boundary condition at the critical point. This condition is that the right-hand side of equations 7 and 4 vanish for $x = x_{crit}$. Then we integrate the vector we calculated in this way from $x = x_{crit} + dx$ to a very large number (choices from 100 to 1000 for this number do not change the result) to get the value of the perturbation variables towards infinity. The integration is done with a fourth-order Runge-Kutta method.

In order to actually find σ, we use a simple interval bisection method. We start with two values of σ, σ_1 and σ_2, which we consider to bracket the eigenvalue we are looking for. Then we compare the value of the solution we get for each of these sigmasat infinity with the analytical one. If the difference changes sign from σ_1 to σ_2, then it means we have a sigma in this interval for which the difference is zero. We split the interval at the middle and compare the analytical value with the value for $\sigma_3 = (\sigma_1 + \sigma_2)/2$. If the difference is a smooth function of σ, this method should converge to a value of σ for which the solution at infinity matches the analytical one.

4.2. A determinant minimization method

This method is similar in principle to the shooting method described above, in that one needs to integrate the solution from some boundary conditions to the critical point. In this case though, we begin with two linearly independent solutions from $x = 0$ to a point just before the critical point, $x = x_{crit} - dx$, and three linearly independent solutions from infinity to a point just after the critical point, $x = x_{crit} + dx$. The asymptotic form of the solutions at infinity is given by:

$$\begin{aligned} r_{1\infty} &= c_3 \rho_0 x^\sigma \\ u_{1r\infty} &= c_4 x^\sigma \\ u_{1\theta\infty} &= c_5 x^\sigma \\ \Phi_{1\infty} &= r_1 x^2/(-\sigma(-\sigma - 1) - l(l+1)) \end{aligned}$$

for the Larson-Penston solution. By choosing different combinations of c_3, c_4 and c_5 we obtain the three linearly independent solutions we need from infinity. We then construct a matrix, composed of the values of the five independent vectors at the critical point, $S_i = (r_{1i}, u_{1ri}, u_{1\theta i}, \Phi_{1i})$ and look at the value of the determinat of this matrix for different values of σ.

This principle is combined with an optimization method, which is an implementation of the Brent function minimization algorithm. The algorithm receives an initial interval bracketed by three values of σ, which in our implementation is provided by a "golden ratio" bracketing algorithm, and looks for a minimum of the absolute value of the determinant by fitting parabolae to the points provided by the determinant calculation module.

4.3. A relaxation method

This code, written and provided for this project by Pascale Garaud, is an implementation of the Newton-Raphson-Kantorovich algorithm. This algorithm is commonly used to solve equations of coupled ordinary differential equations.

The probelm in this case needs to be posed as a two-point boundary problem. The method starts from a guess of the values of the functions on a monotonically increasing or decreasing mesh and adding a correction to the values at each iteration, until the relative error falls below the required tolerance.

This method, providing a completely different approach to the problem, can not only validate our findings from the two previous strategies, but maybe also locate multiple eigenvalues for a certain mode, something difficult to achieve with the two previous methods.

5. Results

The shooting method, as used by HM99, has been implemented succesfully to reproduce the result quoted in Hanawa & Matsumoto (2000) almost exactly, namely a growth rate of $\sigma = 0.37$ instead of the $\sigma \simeq 0.325$ we can induce from Figure 2 of that paper. We found the result to depend on the distance dx we chose to keep from the critical point, on the accuracy of the Runge-Kutta integration and very losely on the distance from zero and the large number we set to represent infinity. Convergence depends on the initial guess of the interval, $[\sigma_1, \sigma_2]$. In accordance to HM99, we found no higher unstable modes.

The determinant minimization method has also been implemented in a numerical code and is currently being tested for potential errors using the singular solution with a constant perturbation. The tests so far give a growth rate of $\sigma = -0.9$, close to one of the known values for σ, -1, but at an error that indicates a fault in the implementation.

We are also currently adapting the code that the Newton-Raphson-Kantorovich method to fit this problem. Although all the relevant routines have been altered, it seems that the code is still not able to solve the ODE system. This probably relates to the existence of a critical point in the equilibrium solution, in which case we could treat it with a remaping of the mesh, leaving the critical point at one of the boundaries, or it is caused by an error in the implementation of the equations.

6. Outlook

During the six weeks of the ISIMA project we managed to derive the perturbation equations in the comoving frame of the collapse, in physical coordinates, for the restricted and for the full perturbation. We have also developed two different numerical codes and adapted a third one for solving this problem using different strategies: a shooting method, following HM99, a minimization method for the determinant of the eigenvector matrix and a relaxation method based on the Newton-Raphson-Kantorovich algorithm.

We have completed and tested the code which performs the shooting method for the restricted problem and managed to reproduce the results obtained with the same method by Hanawa & Matsumoto (2000), additionally finding a second, slower growth rate for the l=2 perturbation, equal to -0.2. The minimization code is still in the testing process and the relaxation code still needs to be further adapted for treating solutions with critical points. Once these tasks are complete, we can continue exploring the dispersion relation for higher perturbation modes and perform the same analysis for the full perturbation, including the oscillatory modes.

Eventually, we would like to complete this work by looking at the problem with a polytropic equation of state for the gas, which is a better approximation for the collapse of a pre-stellar core. Moreover, we would like to complement our findings with numerical simulations of gravitational collapse using the hydrodynamical code RAMSES (Teyssier 2002).

REFERENCES

Alves, J., Lombardi, M., & Lada, C. J. (2007). The mass function of dense molecular cores and the origin of the IMF. *A&A*, **462**, L17–L21.

Bate, M. R. & Bonnell, I. A. (2005). The origin of the initial mass function and its dependence on the mean Jeans mass in molecular clouds. *MNRAS*, **356**, 1201–1221.

Chabrier, G. & Hennebelle, P. (2010). Star Formation: Statistical Measure of the Correlation between the Prestellar Core Mass Function and the Stellar Initial Mass Function. *ApJ*, **725**, L79–L83.

Elmegreen, B. G. & Scalo, J. (2004). Interstellar Turbulence I: Observations and Processes. *ARA&A*, **42**, 211–273.

Girichidis, P., Federrath, C., Banerjee, R., & Klessen, R. S. (2011). Importance of the initial conditions for star formation - I. Cloud evolution and morphology. *MNRAS*, **413**, 2741–2759.

Goodwin, S. P., Kroupa, P., Goodman, A., & Burkert, A. (2007). The Fragmentation of Cores and the Initial Binary Population. *Protostars and Planets V*, pages 133–147.

Hanawa, T. & Matsumoto, T. (1999). Growth of a Bar Perturbation during Isothermal Collapse. *ApJ*, **521**, 703–707.

Hanawa, T. & Matsumoto, T. (2000). Stability of a Dynamically Collapsing Gas Sphere. *PASJ*, **52**, 241–+.

Larson, R. B. (1969). Numerical calculations of the dynamics of collapsing proto-star. *MNRAS*, **145**, 271–+.

Matzner, C. D. & McKee, C. F. (2000). Efficiencies of Low-Mass Star and Star Cluster Formation. *ApJ*, **545**, 364–378.

Maury, A. J., André, P., Hennebelle, P., Motte, F., Stamatellos, D., Bate, M., Belloche, A., Duchêne, G., & Whitworth, A. (2010). Toward understanding the formation of multiple systems. A pilot IRAM-PdBI survey of Class 0 objects. *A&A*, **512**, A40+.

Penston, M. V. (1969). Dynamics of self-gravitating gaseous spheres-III. Analytical results in the free-fall of isothermal cases. *MNRAS*, **144**, 425–+.

Shu, F. H. (1977). Self-similar collapse of isothermal spheres and star formation. *ApJ*, **214**, 488–497.

Teyssier, R. (2002). Cosmological hydrodynamics with adaptive mesh refinement. A new high resolution code called RAMSES. **385**, 337–364.

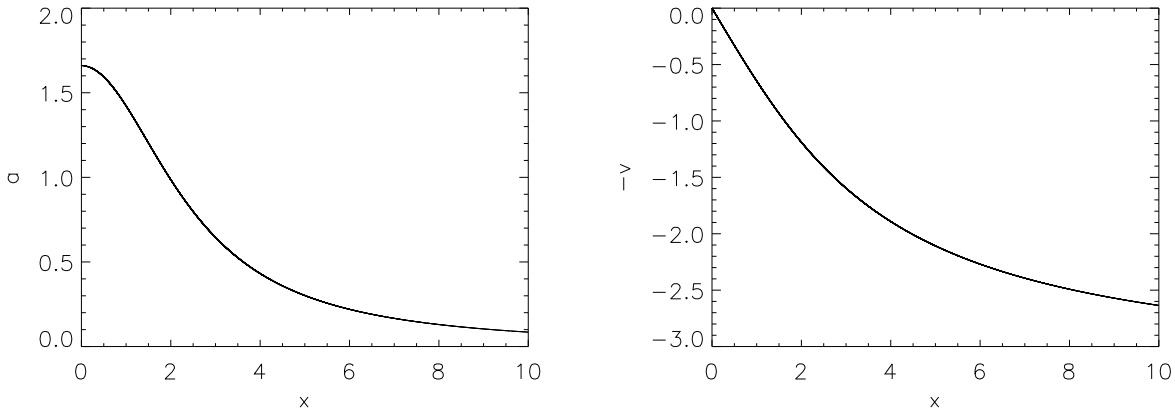

Fig. 2.— The Larson-Penston collapse solution. Left: density profile. Right: velocity profile.